Thermodynamics of oxygen defective TiO_{2-x} : The Magneli phases.

Leandro Liborio

Giuseppe Mallia

Nicholas Harrison

Computational Materials Science Group

Imperial College London

Magneli Phases

Figure 1a

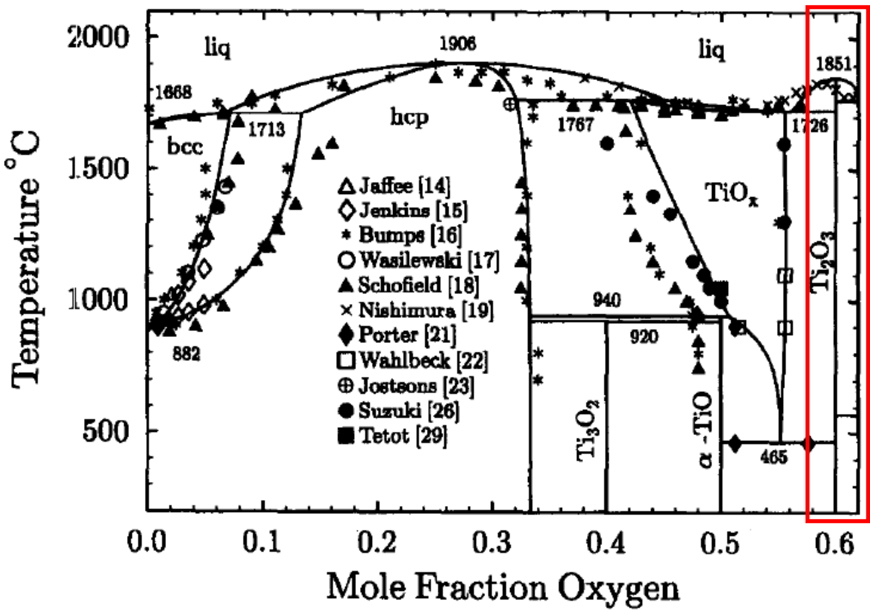

Figure 1b

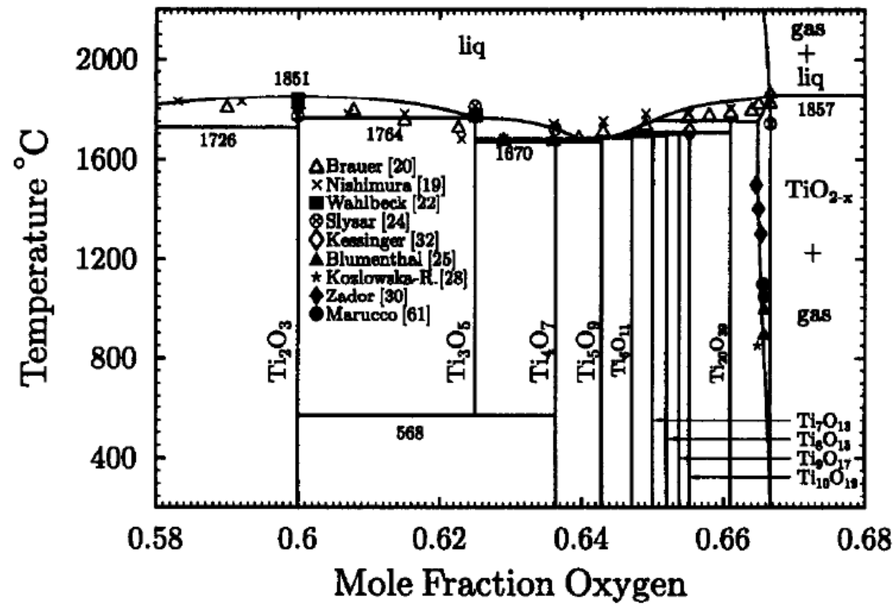

T_nO_{2n-1} composition, $4 \le n \le 9$ .Oxygen defects in {121} planes.

Ti_4O_7 at T<154K insulator with 0.29eV band gap(1).

T_4O_7 Metal-insulator transition at 154K, with sharp decrease of the magnetic susceptibility.

(1) K. Kobayashi *et al*., Europhysics Lett., Vol. 59, pp. 868-874, 2002.

(2) W. Masayuki *et al*., J. of Luminiscence, Vol. 122-123, pp. 393-395, 2007.

(3) P. Waldner and G. Eriksson, Calphad Vol. 23, No. 2, pp. 189-218, 1999.

Magneli Phases: T_4O_7 crystalline structure

Figure 3a

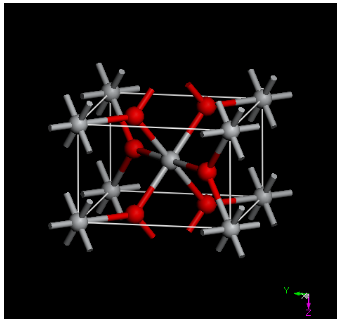

Rutile unit cell

Figure 3b

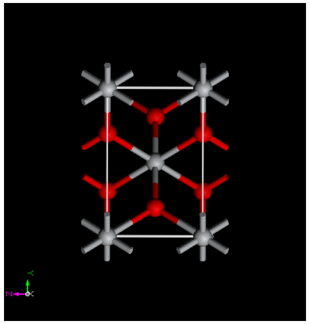

View along the **a** lattice parameter

Figure 3c

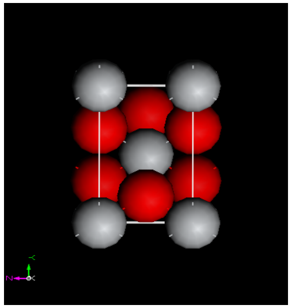

View of Hexagonal oxygen arrangement

Figure 3d

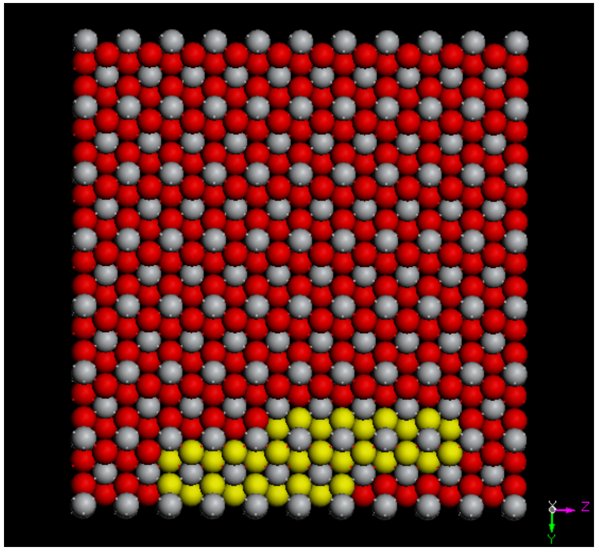

View of Hexagonal oxygen network

Figure 3e

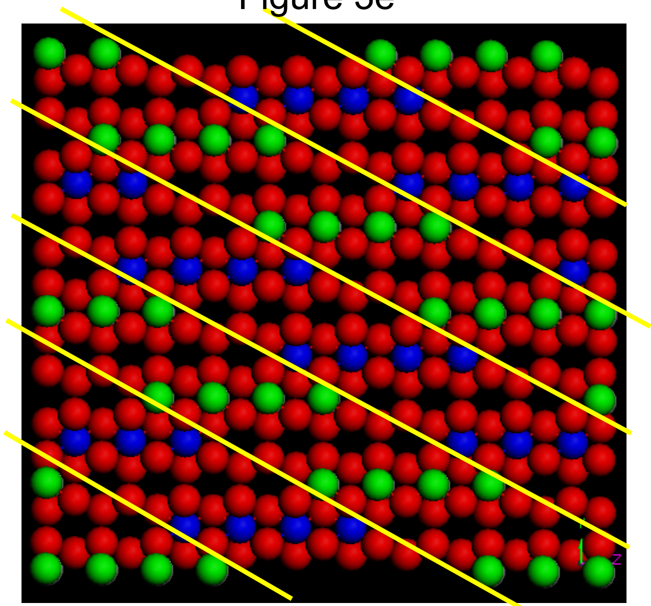

Metal nets in antiphase. $(121)_r$ Cristallographic shear plane.

Technical details of the calculations

CASTEP

Local density functional: LDA

Ultrasoft pseudopotentials replacing core electrons

Plane waves code

Supercell approach

Simulated systems: Oxygen point-defective supercell, Magneli phases supercells, Titanium bulk metal.

CRYSTAL

Hybrid density functional: B3LYP,
GGA Exchange
GGA Correlation
20% Exact Exchange

All electron code. No pseudopotentials

Local basis functions: atom centred Gaussian type functions.
Ti: 27 atomic orbitals, O: 18 atomic orbitals

Supercell approach

Simulated systems: Oxygen point-defective supercell, Magneli phases supercells, Oxygen molecule.

Defect Formation Energies: Thermodynamical Formalism

Figure 5a

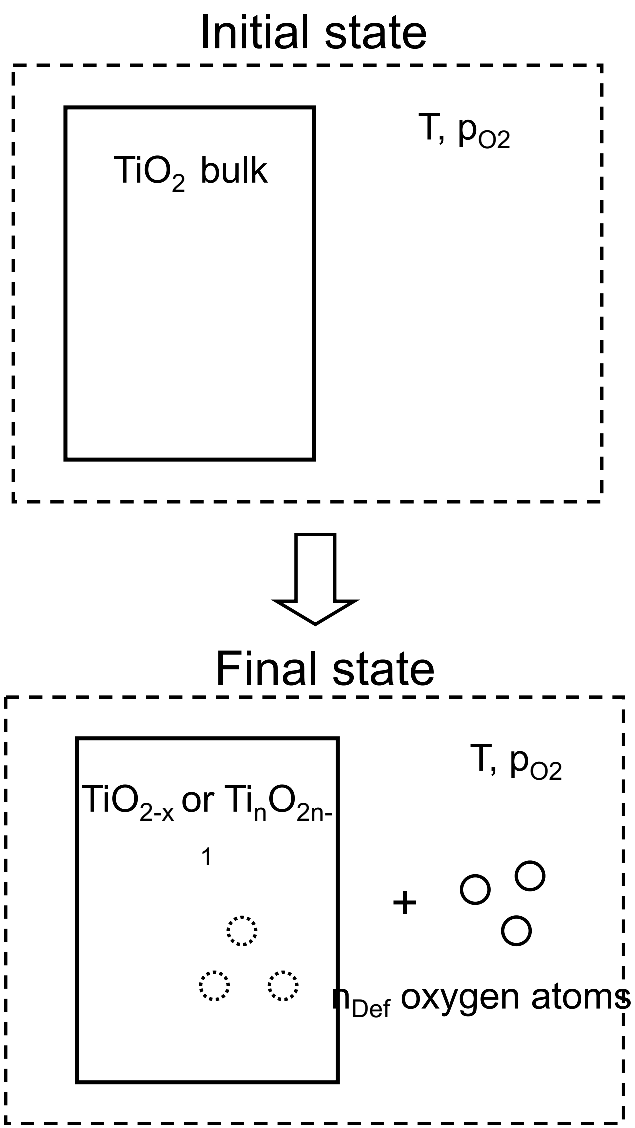

$$\Delta G_f^{Def}(T,p_{O_2}) = \frac{1}{n_{TiO_2}}\left(G^{\text{supcell}}(T,p_{O_2}) + n_O^{Def}\mu_O^{ref}(T,p_{O_2})\right) - \frac{1}{n_{TiO_2}}\left(n_{TiO_2}\mu_{TiO_2}^{bulk}(T,p_{O_2})\right) \qquad (1)$$

$$\Delta G_f^{Def}(T,p_{O_2}) = \frac{1}{n_{TiO_2}}\left(E^{\text{supcell}}(0K) - n_{TiO_2}E_{TiO_2}^{bulk}(0K)\right) +$$

Phonon contribution $+\frac{1}{n_{TiO_2}}\left(F_{Vib}^{\ \text{supcell}}(T) - n_{TiO_2}F_{Vib\,TiO_2}^{bulk}(T)\right) +$

pV contribution $+\frac{1}{n_{TiO_2}}p_{O_2}\left(V_{Vib}^{Supcell} - n_{TiO_2}V_{TiO_2}^{bulk}\right) +$

$$+\frac{n_O^{Def}}{n_{TiO_2}}\mu_{O_2}^{ref}(T,p_{O_2}) \qquad (2)$$

$$\Delta G_f^{Def}(T,p_{O_2}) = \frac{1}{n_{TiO_2}}\left(E^{\text{supcell}}(0K) - n_{TiO_2}E_{TiO_2}^{bulk}(0K)\right) + \frac{n_O^{Def}}{n_{TiO_2}}\mu_O^{ref}(T,p_{O_2}) \qquad (3)$$

Defect Formation Energies: Oxygen chemical potential

$$\Delta G_f^{Def}(T, p_{O_2}) = \frac{1}{n_{TiO_2}}\left(E^{\sup cell}(0K) - n_{TiO_2} E_{TiO_2}^{bulk}(0K)\right) + \frac{n_O^{Def}}{n_{TiO_2}} \mu_O^{ref}(T, p_{O_2}) \qquad (3)$$

Limits for the oxygen chemical potential:

$$E_0 + \frac{\Delta G_f^{Rutile}(T^0, p_{O_2}^0)}{2} \leq \mu_O(p_{O_2}, T) \leq E_0 \quad (4)$$

Hard limit

Soft limit

Assuming the oxygen behaves as an ideal gas:

$$\mu_{O_2}(p_{O_2}, T) = 2\mu_O(p_{O_2}, T) = E_0 + (\mu_{O_2}^0 - E_0)\frac{T}{T^0} - \frac{5k}{2} T \ln\left(\frac{T}{T^0}\right) + kT \ln\left(\frac{P_{O_2}}{P_{O_2}^0}\right) (5)$$

Oxygen molecule's total energy at 0K

Oxygen molecule's standard chemical potential at T=298K and p_{O2}=1atm

Expression (5) allows the calculation of $\mu^0_{O2}(T, p_{O2})$ at any T and p_{O2}

Oxygen chemical potential

CASTEP

$$\mu^0_{O_2}(p^0,T^0)=\frac{2}{y}\left(\mu^{bulk}_{M_xO_y}-x\mu^{bulk}_{M}-\Delta G^0_{M_xO_y}(p^0,T^0)\right)$$

M_xO_y: ZnO, Anatase, Rutile, Ti_4O_7, Ti_3O_5

$\mu^0_{O2}(T^0, p^0_{O2}) = \mu_{mean} \pm \Delta\mu$

Now E_0 has to be calculated

CRYSTAL

E_0 and the 0K total energy of the oxygen atom are calculated with CRYSTAL.

	Exp.	PW-GGA (4)	CRYSTAL
Binding energy [eV]	2.56	3.6	2.53
Bond length [ang]	1.21	1.22	1.23

Now μ^0_{O2} has to be calculated

$$\mu_{O_2}(p^0_{O_2},T)=A(T-T\ln(T))-\frac{1}{2}\mathrm{B}T^2-\frac{1}{6}\mathrm{C}T^3-\frac{1}{12}\mathrm{D}T^4-\frac{\mathrm{E}}{2\mathrm{T}}+\mathrm{F}-\mathrm{G}T \quad (6)$$

T>298K and p_{O2}=1atm

$$\mu_{O_2}(p_{O_2},T)=E_0+(\mu^0_{O_2}-E_0)\frac{T}{T^0}-\frac{5k}{2}T\ln\left(\frac{T}{T^0}\right)+kT\ln\left(\frac{P_{O_2}}{P^0_{O_2}}\right) \quad (5)$$

T>0K and any p_{O2}

(4) W. Li *et al.*, PRB, Vol. 65, pp. 075407-075419, 2002.

Results for the Magneli phases

Figure 8a

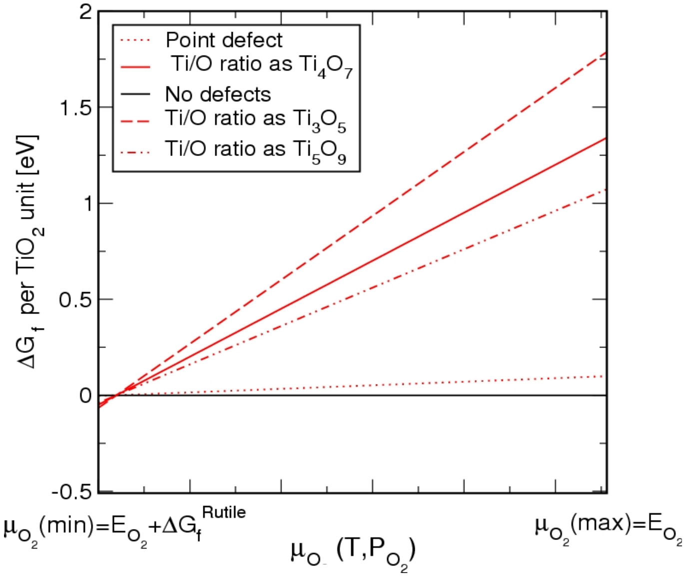

Figure 8b

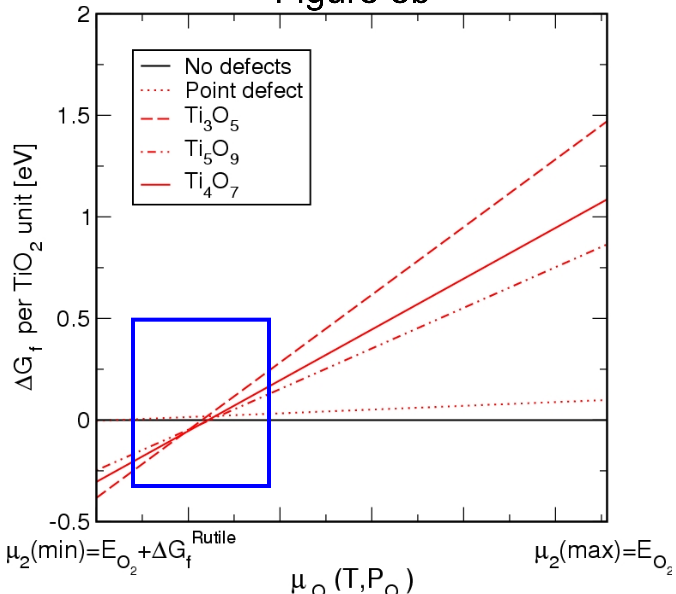

Isolated defects

$$\Delta G_{f\ isolat.}^{Def}(T,p_{O_2})=\frac{n_O^{Def}}{n_{TiO_2}}\left(E^{supcell}(0K)-n_{TiO_2}E_{TiO_2}^{bulk}(0K)+\mu_O^{ref}(T,p_{O_2})\right)$$

$$\left(\frac{n_O^{Def}}{n_{TiO_2}}\right)_{T_4O_7}=\frac{1}{4}$$

$$\Delta G_{\left(\frac{Ti}{O}\right)\text{like } Ti_4O_7}^{Def}(T,p_{O_2})=\frac{1}{4}\left(E^{Supcell}(0K)-27E_{TiO_2}^{bulk}(0K)+\mu_O^{ref}(T,p_{O_2})\right)$$

Magneli phases

$$\Delta G_f^{Def}(T,p_{O_2})=\frac{1}{n_{TiO_2}}\left(E^{supcell}(0K)-n_{TiO_2}E_{TiO_2}^{bulk}(0K)\right)+\frac{n_O^{Def}}{n_{TiO_2}}\mu_O^{ref}(T,p_{O_2})$$

$$\left(\frac{n_O^{Def}}{n_{TiO_2}}\right)_{T_4O_7}=\frac{1}{4}$$

$$\Delta G_{Ti_4O_7}^{Def}(T,p_{O_2})=\frac{1}{16}\left(E^{Ti_4O_7}(0K)-8E_{TiO_2}^{bulk}(0K)\right)+\frac{1}{4}\mu_O^{ref}(T,p_{O_2})$$

Results for the Magneli phases

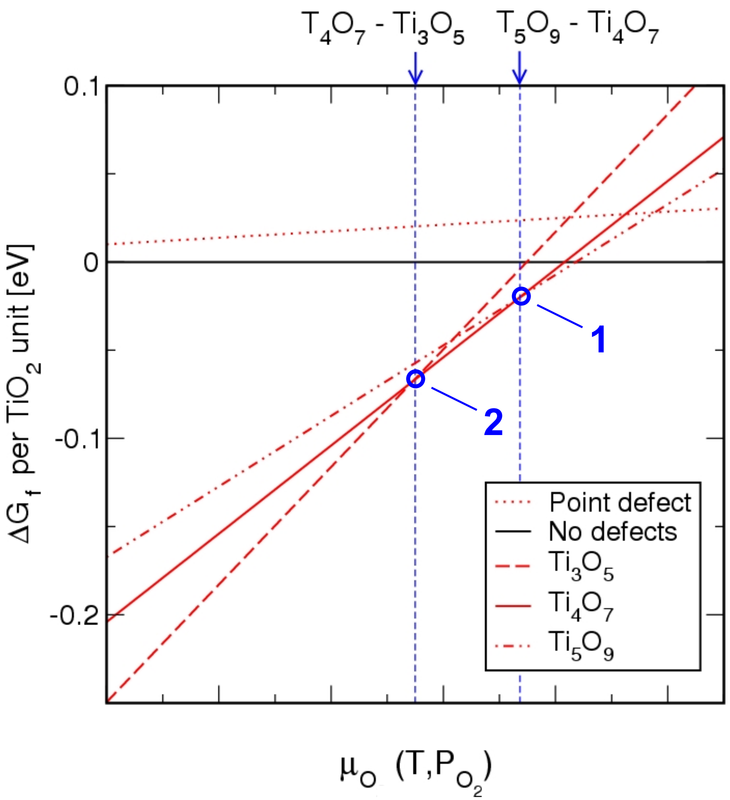

$$\Delta G^{Def}_{Ti_3O_5}(\mu_O) = K_{Ti_3O_5} + \frac{\mu_O}{3}$$

$$\Delta G^{Def}_{Ti_4O_7}(\mu_O) = K_{Ti_4O_7} + \frac{\mu_O}{4}$$

$$\Delta G^{Def}_{Ti_5O_9}(\mu_O) = K_{Ti_5O_9} + \frac{\mu_O}{5}$$

Equilibrium point 1:

$$\Delta G^{Def}_{Ti_4O_7}(\mu_O) = \Delta G^{Def}_{Ti_5O_9}(\mu_O) \Rightarrow \mu^{eq}_{Ti_4O_7 - Ti_5O_9}$$

Equilibrium point 2:

$$\Delta G^{Def}_{Ti_4O_7}(\mu_O) = \Delta G^{Def}_{Ti_3O_5}(\mu_O) \Rightarrow \mu^{eq}_{Ti_4O_7 - Ti_3O_5}$$

$$\mu^{eq}_{Ti_4O_7 - Ti_5O_9} = \mathrm{E}_0 + (\mu^0_{O_2} - E_0)\frac{T}{T^0} - \frac{5k}{2}T\ln\left(\frac{T}{T^0}\right) + kT\ln\left(\frac{P_{O_2}}{P^0_{O_2}}\right)$$

Relationship between p_{O2} and T in the phase equilibrium.

Results for the Magneli phases

Figure 10a

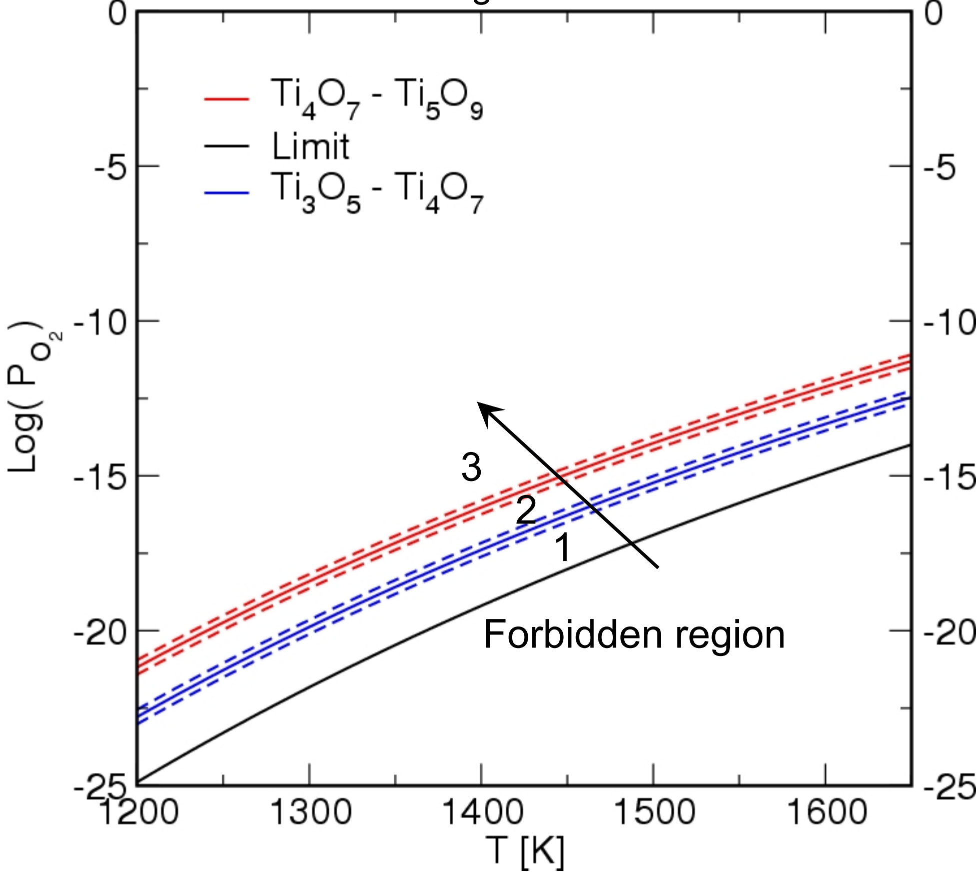

1 → 2 → 3

$Ti_3O_5 \rightarrow Ti_4O_7 \rightarrow Ti_5O_9$

Figure 10b

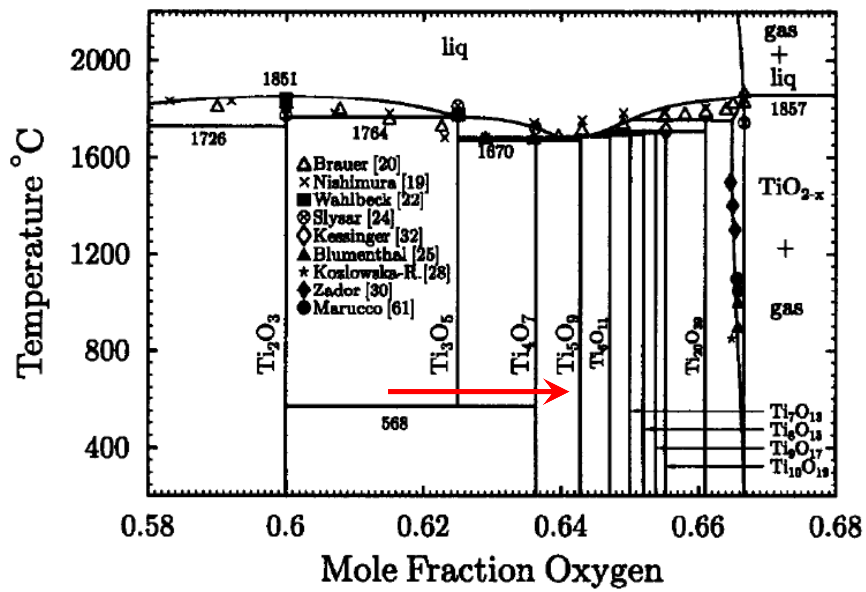

$$\log_{10}\left(p_{O_2}\right) = \frac{K^{eq}_{Ti_4O_7-Ti_5O_9}}{T} + K_1 \ln\left(\frac{T}{T^0}\right) + K_2$$

(1) P. Waldner and G. Eriksson, Calphad Vol. 23, No. 2, pp. 189-218, 1999.

CASTEP Results for the Magneli phases

Figure 10a

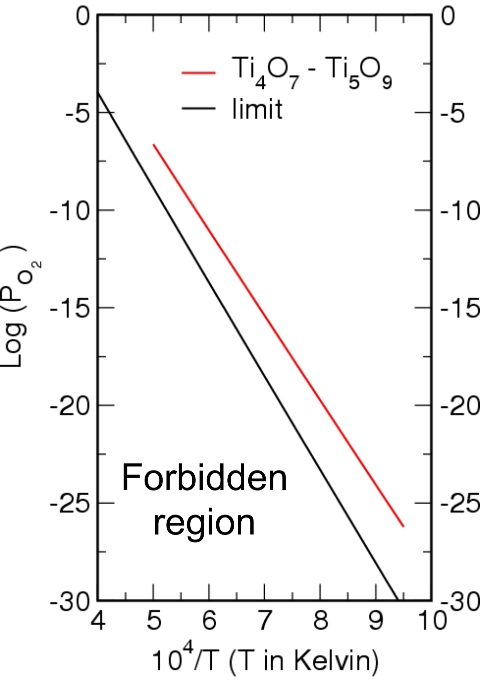

Figure 10b

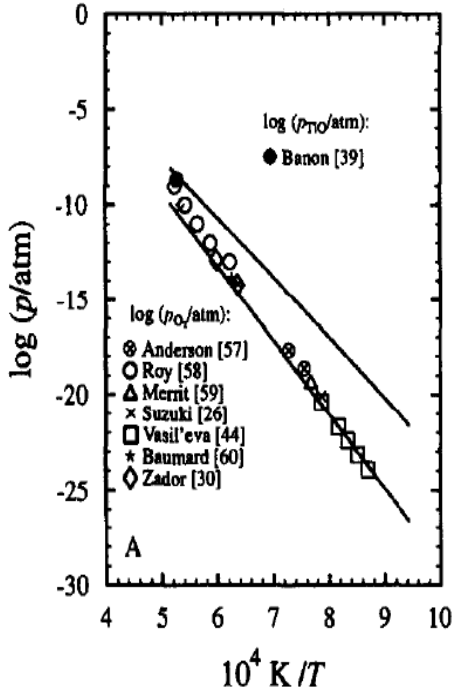

Figure 10c

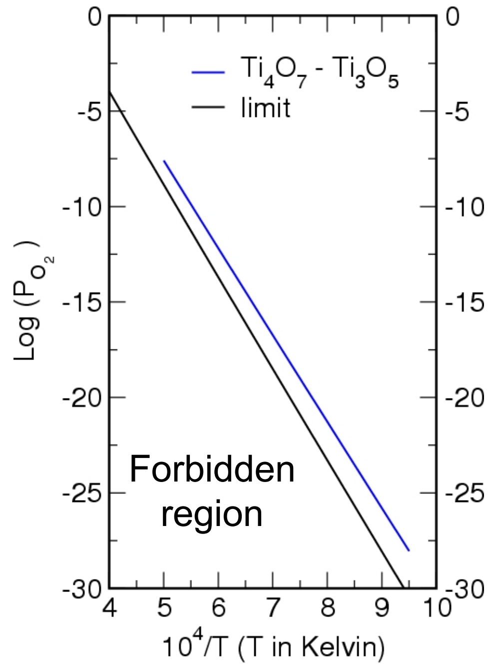

Figure 10d

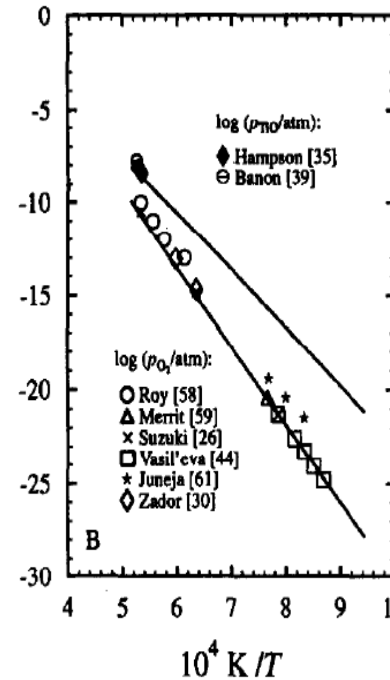

(1) P. Waldner and G. Eriksson, Calphad Vol. 23, No. 2, pp. 189-218, 1999.

CRYSTAL Results for the Magneli phases

Figure 12a

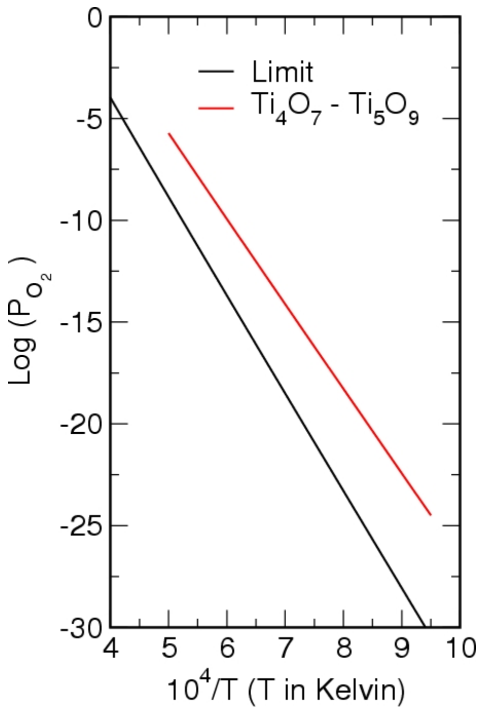

Figure 12b

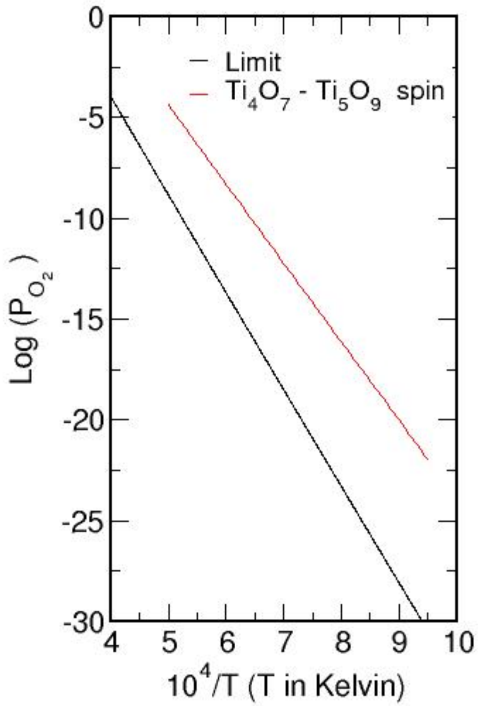

Figure 12c

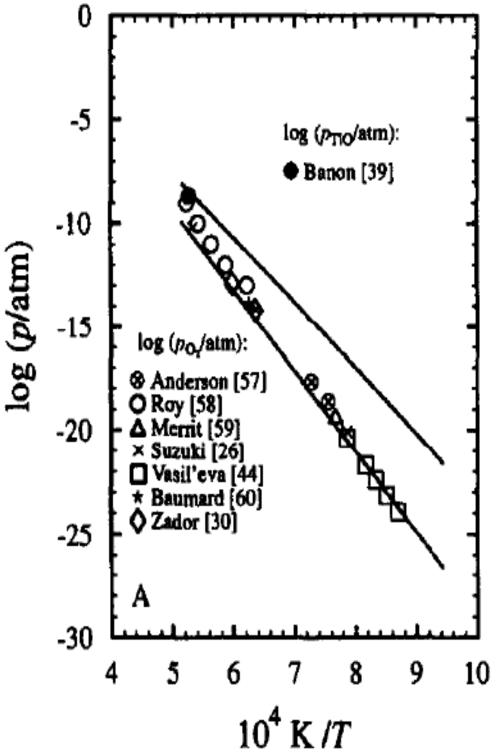

P. Waldner and G. Eriksson, Calphad Vol. 23, No. 2, pp. 189-218, 1999.

Formation mechanism for an oxygen-defective plane

Cation + anion (100) layer

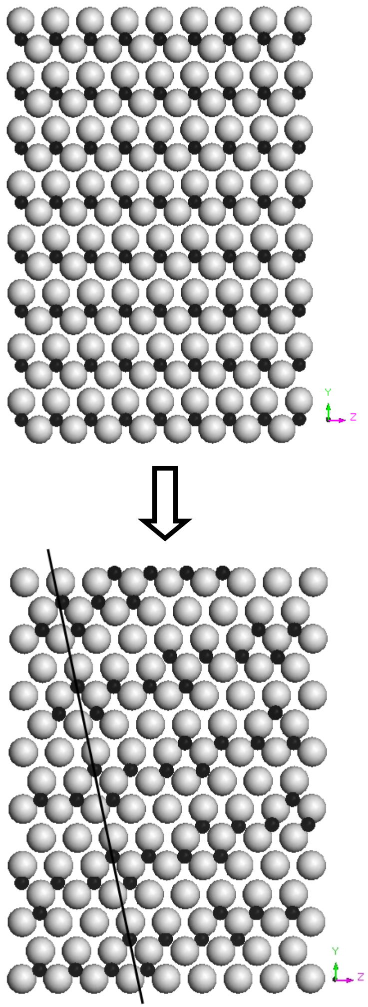

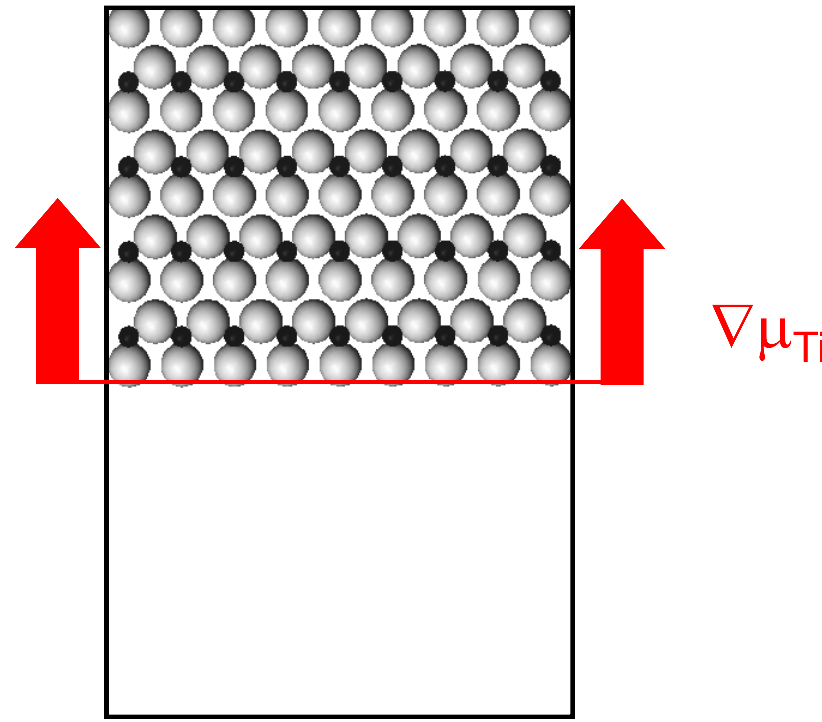

$$\mu_{TiO_2}^{bulk} = \mu_{Ti}^{supercell} + 2\mu_O^{ref}(p_{O_2}, T)$$

L. Bursill and B. Hyde, Prog. Sol. State Chem. Vol. 7, pp. 177, 1972.

S. Andersson and A. D. Waldsey, Nature Vol. 211, pp. 581, 1966.

Formation mechanism for an oxygen-defective plane

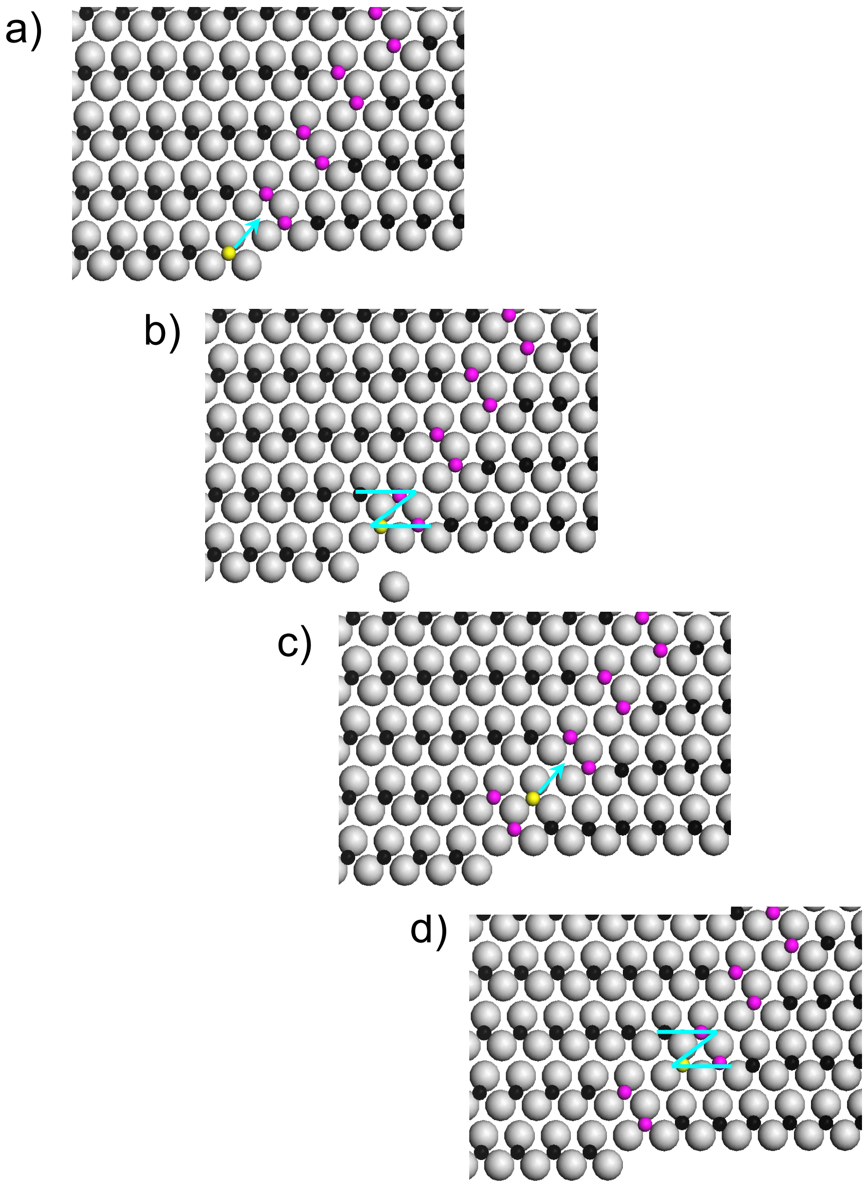

Final stages

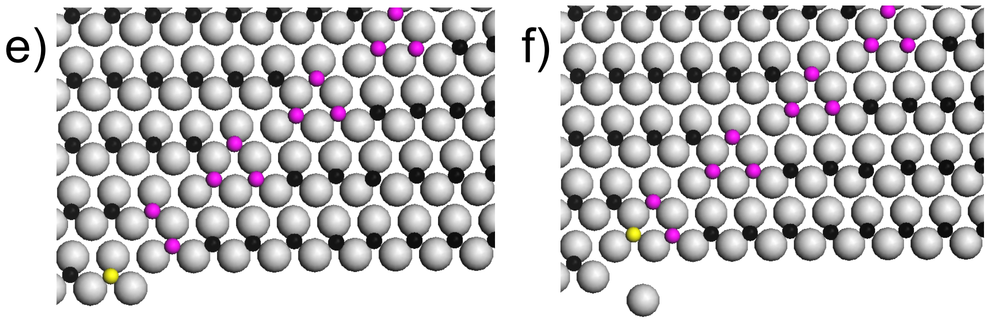

- Antiphase boundaries (dislocation) acts as high conductivity paths for titanium.
- Dislocations are needed
- No long-range diffusion
- Formation of Ti interstitials.

Conclusions

•The thermodynamics of rutile's higher oxides has been investigated by first principles calculations.

•First principles thermodynamics reproduce the experimental observations reasonably well.

•Spin does not affect the thermodynamics.

•At a high concentration of oxygen defects and low oxygen chemical potential, oxygen defects prefer to form Magneli phases.

•But, at low concentration of oxygen defects and low oxygen chemical potential, titanium interstitials proved to be the stable point defects.

•These results support the mechanism proposed by Andersson and Waldsey for the production the crystalline shear planes in rutile.

Acknowledgements

- Prof. Nic Harrison
- Dr. Giuseppe Mallia
- Dr. Barbara Montanari
- Dr Keith Refson